CERN 78-05
Experimental Physics
Division
14 June 1978

ORGANISATION EUROPÉENNE POUR LA RECHERCHE NUCLÉAIRE
CERN EUROPEAN ORGANIZATION FOR NUCLEAR RESEARCH

NEW APPROACHES TO HIGH-RATE PARTICLE DETECTORS

G. Charpak, G. Melchart, G. Petersen and F. Sauli,
CERN, Geneva, Switzerland

E. Bourdinaud and P. Blumenfeld,
DPhPE, CEN Saclay, Gif-sur-Yvette, France

C. Duchazeaubeneix and A. Garin,
DPhME, CEN Saclay, Gif-sur-Yvette, France

S. Majewski and R. Walczak,
Institute of Experimental Physics,
University of Warsaw, Poland

GENEVA
1978

CERN - Service d'information scientifique - RD/337 - 1600 - juin 1978

ABSTRACT

Methods are described for overcoming the limitation, due to space charge, in the detection efficiency of multiwire proportional chambers operated in high particle fluxes. By dividing the gas amplification process into two separate steps, a time interval allows for a fast selection of the detected events. The two schemes of preamplification investigated are a) secondary emission by low-density surfaces followed by electron acceleration in vacuum and detection in a multiwire chamber, and b) gaseous amplification by avalanche formation in a nearly uniform field between wire grids. Tests have shown the latter method to be capable of good gain with high resolution, which should permit the reduction of the space-charge limit of wire chambers by several orders of magnitude.

DD-PUB/kw-mg-msv-mg

CONTENTS

1. INTRODUCTION

In recent years, several experiments have been seriously limited in their data-taking rate by the degradation of multiwire proportional chamber (MWPC) performances at high fluxes. There are two main factors that contribute to determining the maximum rates at which this class of detectors can be employed efficiently: the finite resolution and memory times, and the decrease of gain due to space-charge build-up. Although the resolution time in a good MWPC with 2 mm anode wire spacing is of about 30 nsec, the amount of accidental coincidences is mainly determined by the collection time of electrons from the drift region. For an 8 mm gap, as used in most large-size chambers, some electrons are collected, delayed by as much as 200 nsec with respect to the fast ones.

In other words, at rates around 10^7 sec^{-1} the accidentals represent the majority of the detected events even if validation gates as short as the chamber resolution are used. The addition of electronegative vapours in the gas, by reducing the effective memory times, improves the issue only slightly[1]. The space-charge build-up is an even more severe limitation to the operation at high rates[2]. The positive ions produced in the avalanche process migrate only slowly to the cathodes, and the charge accumulation that follows strongly modifies the electric field in the counter and hence its performance. At a particle rate of 10^4 mm^{-1} sec^{-1}, a gain reduction exceeding 50% has been measured at usual values of the multiplication factor[3], with a consequent decrease in the detection efficiency. Since, at least in first approximation, the gain reduction depends exponentially on the multiplication factor, the operation of counters at low gains would improve their rate capability, but in practice this implies the use of prohibitively low threshold electronic discrimination.

In the following we will describe a possible way of overcoming the quoted rate limitations in MWPCs by a drastic change in their mode of operation.

2. PRINCIPLE OF THE METHOD

With reference to Fig. 1, the principle of the method is as follows. The amplification process leading to an over-all gain M is split into two independent steps: an amplification by a factor M_1 in the region A_1, and by M_2 in A_2, such that $M = M_1 \cdot M_2$. The two regions A_1 and A_2 are separated by a drift region D, such that electrons produced in A_1 reach A_2 after a time T_D.

At the far end of region D a physical gate G (which we will describe later) may collect the electrons from D or let them be transferred to A_2. Such a physical gate plays the following role: if the event is not acceptable the electrons produced in A_1 will be collected at the end of D and not permitted to enter A_2. If the event is validated by external detectors and rapid electronic analysis, a gate of delay equal to T_D and of suitable width will transfer the electrons to A_2, which in this study, is a MWPC.

When a charged particle traverses the detector, a series of electrons are produced in A_1, A_2, and D, and the following phenomena occur:

Detection in the multiwire chamber A_2: The gain is reduced by a factor M_1 with respect to a normally operating chamber. Owing to the above-mentioned very fast exponential dependence of the positive space-charge effects from the gain, the limits in the direct chamber detection will be encountered at fluxes several orders of magnitude larger than normal, depending on

the actual value of M_2. Conditions are chosen such that pulses from direct detection of charged tracks are below the discrimination threshold of the read-out electronics of A_2. We want to accept in A_2 only selected events, which may be rare, and these have been preamplified in such a way by A_1 as to be detectable in A_2.

Multiplication in the preamplification region A_1: This provides a preamplification by a factor M_1 to all tracks. Obviously this is a key part of the scheme, and in the following section we will describe two possible ways of implementing this function.

Selection of valid events: The drift space D serves a double purpose. It delays the swarm of electrons coming from A_1 by a constant time, thus allowing a logical decision to be made on the acceptance of the tracks, and it contains a controlled electronic gate at its end to forbid all but the electrons from selected events to enter the proportional chamber A_2. In conditions that are typical for the operation of gas counters, the delay T_D can be of the order of 200 nsec for a 10 mm long drift length. Classic solutions exist for implementing the electronic gate G, either by using a pulsed inversion of electric field between two meshes or by applying alternated potentials to adjacent wires so as to collect all electrons. The electronic transparency is then restored by a voltage pulse that brings the mesh to an equipotential[4] (Fig. 2).

We have experimented with both solutions. In the case illustrated by Fig. 2a, two fine wire meshes, 1.6 mm apart and having 85% optical transparency, were rendered completely opaque to electrons by using a small inverted continuous field of about 60 V cm^{-1} (V_0 = -10 V); by applying a 100 nsec voltage pulse V_0' of about 80 V, of the opposite polarity, a 70% electronic transparency has been measured during the pulsing time. For the scheme depicted in Fig. 2b, and with 1 mm wire spacing in the control grid, a difference of potential of about 400 V appeared to be necessary in order to stop all migrating electrons.

A fundamental limitation in the use of pulsed electric gates resides, of course, in the amount of residual noise pick-up in the active elements of the chamber at the instant of decision. With a small (10 × 10 cm^2) chamber, we have so far achieved a complete recovery of the amplifiers in about 200 nsec using both pulsing methods described, and this corresponds roughly to the drift time from the gate G to the anodes of chamber A_2 (see Fig. 1). Symmetrical pulsing of the alternate wires in the scheme of Fig. 2b reduces the pick-up problems significantly. There is certainly more to be done to bring the level of parasitic pulses to a value where cathode strips, for instance, could easily be read out for a comfortable use of the centre-of-gravity method of coordinate determination. Since our tests were performed without strict construction precautions, their results are quite encouraging.

The time resolution can be set either by the opening time of the gate or by the intrinsic resolution of the proportional chamber A_2. Its minimum value is set by the fluctuation in timing introduced by A_1 and D for particles at different spatial positions. On the assumption (which may be rather optimistic) that the opening time corresponds to the acceptance into the proportional chamber of all (and only) the charges produced by the preamplification element A_1, the total charge liberated in A_2 at a particle flux N, if n is the validated rate, is proportional to

$$N M_2 \left(1 + \frac{n}{N} f M_1\right) ,$$

where f is the ratio of primary charges liberated in region A_1 to those liberated in A_2. If the fraction of accepted events is small, the reduction in the total liberated charge is therefore proportional to M_2.

3. DIFFERENT APPROACHES TO THE PREAMPLIFICATION PROBLEM

We will describe two distinct approaches to the most delicate problem of this undertaking. Both yield promising results and may find distinct applications in different fields.

3.1 Preamplification by secondary emission and electron acceleration in vacuum

Charged particles crossing low-density KCl or CsI surfaces[5-7] emit secondary electrons. These surfaces are prepared under special conditions; essentially, evaporation of successive layers under a low pressure of argon. The density of the deposits is of the order of 1% of the density of the respective solid, and a typical geometrical thickness of 100 μm results in an equivalent thickness of only 1 μm of dense material.

The secondary electrons ejected from such a surface must be extracted under vacuum by an electric field, typically of 20 kV/cm. Recent progress has shown that with minimum ionizing particles it is possible to eject, on the average, around 5-6 electrons and reach 90% efficiency for the detection of the relativistic particles by detecting the secondary electrons[6,7]. However, this factor of 5 is quite insufficient for our purpose and is subject to large fluctuations. We obtain the additional gain by using the extraction field to accelerate the secondary electrons in vacuum and inject them into a proportional chamber after traversal of a thin window. Let R be the residual range of the electrons after entering the chamber. For 10 keV we may expect a ratio of at least two orders of magnitude between the amount of energy deposited by the primary particle in a gas layer of thickness R and the amount of energy deposited by the secondary electrons entering the chamber with this energy.

To check the feasibility of such a scheme, we have constructed the chamber illustrated in Fig. 3. Ten layers of CsI have been evaporated on a thin aluminium support, providing a total thickness of 150 μm of low-density secondary emitter. At a distance of 33 mm, a 2.5 μm thick mylar window separates the acceleration region from a drift space D followed by a conventional MWPC. The entrance window is coated on both sides by a vacuum-evaporated, 0.5 μm aluminium layer, and is supported by a thin wire mesh.

The pressure in the acceleration space is reduced to about 10^{-3} Torr by continuous pumping, and under these conditions up to 30 kV could be applied across the gap without breakdown. This voltage is used to extract the electrons from CsI and accelerate them towards the entrance window of the gas detector. Tests were made with minimum ionizing electrons from a ^{106}Ru source placed above the secondary-emitter layer; fast electrons from the source traversed the chamber and were detected in a pair of scintillation counters, providing the trigger signal.

At low values of the accelerating potential V_A, only a direct signal is observed in the proportional chamber, corresponding to the electron collection from the chamber itself and from the drift space. At a threshold value of about 13 kV, the detection of a pulse begins with the expected delay of about 700 nsec, corresponding to 34 mm of drift in the gas. A further increase in V_A results both in an increase in the delayed signal pulse height and in a decrease in the drift time corresponding to the longer range of the secondary electrons in the chambers.

Analysis of the height of the delayed pulse offers interesting information. Figure 4 shows a pulse-height distribution of the delayed pulses for various accelerating voltages; the average energy loss in the peak, at 25 kV, corresponds to about 10 keV. Since for every electron we expect an energy of about this value, the result implies that we are obtaining essentially single electrons from the secondary emitter. Previous work[7] has shown that for electrons crossing a layer of 125 μm at 45°, the average number of electrons is only 1 at 10 kV/cm and reaches 2.5 at 25 kV/cm. We are applying about 7 kV/cm when the acceleration voltage is 23 kV. It is thus not surprising that we extract only one electron and the detection efficiency is 10% at 23 keV. However, our results are encouraging in the sense that we have demonstrated that a single electron produced by a secondary-emission surface can be detected with almost 100% efficiency. This may have applications that are different from the one originally foreseen. By increasing the extraction field and increasing the layer thickness, we have several possibilities of increasing the efficiency.

Measuring the delayed pulse time-distribution at a fixed threshold of detection in the proportional chamber, we observed the spectra shown in Fig. 5. Just above the threshold value in the accelerating potential, the delayed peak has a narrow time-spread of 20 nsec FWHM, corresponding to electronics jitter and geometrical changes in the drift length (due to the window bulging). At higher values of V_A a tail develops towards shorter times, indicating that the residual range of accelerated electrons in the gas approaches a few millimetres or so. In other words, to obtain a good resolution time we should not take the front end of the pulse but the falling edge, corresponding to the entrance position, which is fixed. In all pictures, the background of events at low times corresponds to accidental triggers on the normal ionization trail.

3.2 Gaseous preamplification

Charge amplification factors can easily be obtained in gaseous detectors; the problem is, however, to transfer all or a fraction of the multiplied charge to another part of the structure.

During the early days of multiwire chambers, hybrid systems were designed where the primary ionization in a gas was preamplified in a single-gap wire chamber and the electrons then transferred to a spark chamber[8-10]. The aim was to use the cheaper and at that time routine technology of spark chamber read-out. A schematic view of the preamplification element in a hybrid chamber is shown in Fig. 6 [9]; it differs from a conventional MWPC in that the electric field is not symmetric around the multiplying electrode. Electrons were supposedly multiplying when reaching the neighbourhood of the wires from the upper high field region, and some of them were escaping in the lower field region where they could trigger a new detection element. The transfer mechanism was attributed, at the time, either to some diffusion process during the avalanche multiplication around the wires or to a photon-induced spread. A preliminary set of measurements done in this direction, using a multiwire chamber in place of the spark chamber of the original design, led to very disappointing results: although some preamplified pulses were detected, both the efficiency and the energy resolution were very bad. Addition of a drift space in front of the preamplification region completely changed the issue, and allowed us to understand the real mechanism of preamplification and transfer of charges. Figure 7 shows the equipotentials and field lines around the central electrode structure, such as the one of Fig. 6, for 35 μm thick wires, 0.5 mm apart, and for a field E_1 (upper region) that is three times larger than E_2 (lower region). There are no lines of force

leaving the wires towards the lower field region, and if all the avalanche process takes place in the vicinity of the wires, it would require, for electrons to leak in the lower region, a diffusion against the field by several hundred microns, which is an unlikely process. There remains the possibility of charge spread by photons emitted in the avalanches, in which case very bad localization properties would be expected from this kind of detector. In the framework of the studies on bidimensional read-out of proportional chambers using the cathode-induced pulses[11,12], we have verified that actually this is not the case even for very poorly quenched gases, and avalanches remain very well localized as long as the gains are not too large. Similar results have been obtained by other authors[13]. Figure 8 shows the angular distribution, around a 20 μm anode wire of a proportional counter, of the ions in an avalanche started by a well-localized cluster of ionization electrons. The technique used is described in Ref. 12. We see that at gains of the order of 1000, well above the value we want to reach in A_1, the avalanches do not propagate around the wire, which excludes a propagation mediated by long-range photons.

These facts all led to the following understanding: the hybrid chamber is nothing but a parallel-plate counter, with some escaping field lines. Multiplication takes place more or less uniformly in the whole of the high field region, and the transfer efficiency depends mainly on the ratio of fields E_1/E_2. It is clear, then, why the addition of a drift region before entering the high field space improves the resolution dramatically: the quantizing structure of the "transparent" multiplication region is obliterated by the increase in electron diffusion when approaching the grid. The correctness of this interpretation is confirmed by a recently published work[14] where a parallel-plate proportional chamber is coupled to a spark chamber, and relies precisely on the use of electron avalanches in a uniform field transferred to a spark gap where the conditions of stability and the plateau of counting rates of β particles are much improved by the injection of a large cluster of electrons at a precise distance from the anode.

We have designed and tested a chamber, showing very clearly the phenomena of preamplification and transfer, with a high efficiency for 6 keV X-rays and fast electrons (Fig. 9). The main construction parameters are as follows. A diffusion region is separated from the preamplification region by a wire mesh, 85% transparent; the 40 μm diameter preamplifying wires are 500 μm apart. A transfer and delay space of 3.5 mm follows, and charges are then drifted into a conventional MWPC. In this preliminary design the gating facility was omitted. Low-price charge amplifiers, having a sensitivity of 250 mV/pC and a time constant of 3 μsec *), were connected both to the preamplification grid and to a group of anodes in the proportional chamber. A suitable choice of the operating potentials then allows the structure to be operated as a conventional MWPC with an additional drift space on one side. When, however, the potential difference HV3-HV2 is increased, at a quite well defined threshold value, preamplification if observed for charges produced above the upper wire grid. Figure 10 shows two phases of this transition in the detection of a ^{55}Fe 5.9 keV X-ray source uniformly irradiating the sensitive volume of the chamber. In Fig. 10a the preamplified pulses begin to appear, separated from the normal ones (which correspond to photons converted below the wire grid), and in Fig. 10b a preamplification factor of about 25 is obtained; this value increases

*) The amplifiers were developed at CERN by J.-C. Santiard, and are produced in a thick film hybrid technique by CIT-Alcatel, France.

very quickly with the potential difference HV3-HV2. So far, the highest preamplification factors have been observed with a gas filling of pure argon bubbled through ethyl alcohol at 0°C; the addition of a small amount of CO_2 (2 to 5%) greatly improves the time resolution of the detector, as we will see later, but reduces the maximum safe preamplification before breakdown.

Figure 11 is a summary of the measured preamplification factors for two values of the MWPC anodic potential and a fixed voltage difference in the transfer and diffusion region, and as a function of the voltage applied to the preamplifying grid. All measurements have been done in the quoted argon-alcohol gas mixture; the error bars in the drawing represent the FWHM of the detected 5.9 keV line. The energy resolution is surprisingly good in these conditions; it varies from 25% at the lowest gains to about 15% at preamplification factors of 100. Examples of pulse-height distributions are given in Figs. 12a and 12b for preamplification factors of 7 and 40, respectively; at the lowest gain, the direct 5.9 keV and 3 keV escape peaks are still visible (Fig. 12a), while they have been suppressed in the spectra of Fig. 12b. The uneven distance between the peaks at the higher gain shows that the space-charge limited the proportionality region approaches, which may partly explain the remarkable resolutions obtained.

At preamplification factors of about 100, a charge signal begins to be detectable directly on the multiplying grid (see Figs. 13). The upper trace shows the signal detected on the preamplification grid, and the lower one the charge on the proportional chamber, operated in a pure ionization chamber mode (Fig. 13a) and at increasing anodic potentials (Fig. 13b and 13c). The scope sensitivities are 4 mV and 200 nsec per division in both Fig. 13a and Fig. 13b; in Fig. 13c the conditions are set for full charge multiplication in the MWPC (in this case, the lower trace sensitivity is decreased to 100 mV/division). The influence of the positive ion feedback on the preamplified pulse is clearly visible.

A very important question that is still pending is the actual value of the transfer efficiency of the preamplification element. All we said so far in terms of preamplification refers, of course, to the fraction of charges that manage to reach the MWPC, and not to the total number produced by the preamplification process. The following interpretation is suggested for the peculiar shape of the direct preamplified pulse shown by the upper traces in Figs. 13. A fast swarm of multiplying electrons traverse the preamplification region, and part of them leave it, thus explaining the fast increase and subsequent decrease of the detected signal. Slow positive ions are left behind which induce the slowly decreasing tail (because of the time constant of the amplifier). If this is a correct interpretation, the transfer efficiency would appear to be the ratio of the two fast-induced signals of opposite polarity, about 50% as from the pictures. Such a high transfer efficiency is surprisingly good. On the other hand, Fig. 13a shows that the charges reaching the anodes of the MWPC, operated in a pure collection mode, induce a pulse height which is about one quarter of the preamplification one; the transfer efficiency would then be about 25%. Further analysis of the properties of charge induction in this complex structure is clearly necessary, taking into account the ion velocities, the electronics time response, and the cathode transparency.

A simple threshold discrimination on the direct preamplified pulse and on the delayed pulse in the MWPC allows both efficiency curves and time delay measurements to be obtained. Figure 14 shows a spectrum of the time difference between delayed and fast pulses, measured with a uniform irradiation of the chamber with a 5.9 keV source, at a preamplification factor of about 100. The FWHM of the distribution is 8 nsec.

Some preliminary measurements have been done using also a ^{106}Ru β emitter in an arrangement similar to the one illustrated in Fig. 3. In Fig. 15 the pulse-height spectra of fast electrons and 5.9 keV X-rays are compared, after a preamplification factor of about 100, as detected in the MWPC. The MWPC efficiency as a function of the anodic potential has been measured and is shown in Fig. 16 for several values of the preamplification grid potential, at a fixed discrimination threshold, corresponding to about 0.1 pC on the chamber. Owing to large multiple scattering and γ accidentals, efficiency measurements realized with β emitters cannot reach 100%, but the presence of a comfortable plateau shows that full efficiency is obtained.

Interestingly enough, if the potential in the diffusion region is reduced below HV2 so as to multiply only charges produced in the preamplification region, full efficiency of detection can still be obtained although the plateaux are reduced in length, as shown in Fig. 17; this suggests that for charged tracks that produce distributed charges, the diffusion space may be suppressed with obvious advantages. In the figure, the efficiency of the system for direct detection of tracks in the MWPC (i.e. without preamplification, HV2 = 0) is also shown, and a comfortable region still exists where full rejection of direct signals is possible.

The time-spread in the detection of the preamplified electron pulse was also measured using the proportional chamber. Because of the large variance in the pulse height, due to Landau fluctuations in the energy loss, good timing is obviously more difficult than it is for X-rays since the typical rise-time of the signals is about 100 nsec (see Fig. 13c). The best result obtained so far is shown in Fig. 18, and has been obtained adding $\sim$ 3% CO_2 in the argon-alcohol gas mixture to increase the drift velocity of the electrons and decrease their diffusion; the FWHM of the distribution (time difference between the scintillation counter signal and the delayed, preamplified pulse in the chamber) is about 20 nsec. A 50 nsec wide electronic gate, of the kind discussed in the previous section, would guarantee full efficiency of detection, and represents the time resolution of the system. Further work is in progress to improve this parameter.

4. CONCLUSION. FUTURE PROSPECTS AND APPLICATIONS

Our investigations have shown that the amplification process leading to the detection of particles in a MWPC can be separated into two successive steps, delayed by a time interval permitting the acceptance of events only after some fast logic decision.

Two approaches have been investigated: the first based on secondary emission from a low-density surface and subsequent electron acceleration; the second one based on gaseous amplification.

This last approach has led to a satisfactory solution of the problem of preamplification. Gains up to 500 are easily reached, leading to a perfect separation of the signals from the direct beam and the preamplified electron cluster. The reduction in the space-charge limit, with a proper use of gating grids, should be about proportional to the preamplification factor. Even for moderate rates the approach of preliminary amplification offers attractive features.

The delay of the signal with respect to the passage of the particle is obtained from the chamber without requiring the painful and sometimes expensive methods of electronics or cables.

The wire spacing of a large MWPC has usually to be kept above 2 mm for mechanical reasons and because of the difficulty of reaching proper amplification fields without entering into unstable operation conditions. The pregain of 500 permits a considerable release in the construction constraints, and it becomes as easy to detect minimum ionizing particles as to detect α particles!

An important application, which can readily be foreseen for this technique of preamplification gap associated with a wire chamber, is the reduction of the thickness of the sensitive gas layer in a chamber. It is well known that when one aims at imaging the distribution of electrons emitted by planar sources placed against a wire chamber, the finite range of the electrons in the gas limits the spatial resolution. This is the case for paper chromatography of radioactive sources, or for thermal neutron conversion in gadolinium foils. While it is very difficult to imagine wire chambers of 1 mm thickness, it seems much easier to have a preamplifying space where the sensitive layer is very thin, thus reducing to a negligible value the parallax errors for inclined tracks.

The method used for secondary-electron emission and subsequent acceleration is still far from giving the proper preamplification factor. The different factors which can be optimized do not seem to promise more than one order of magnitude gain in this factor, and full efficiency for minimum ionizing particles is so far not guaranteed. However, here also several promising applications emerge from the preliminary results.

For thermal neutrons, reactions in ^{10}B and ^{6}Li lead, with a very high cross-section, to nuclear fragments. These fragments cannot emerge from layers that are thick enough to obtain full efficiency. However, if low-density surfaces can be made with these substances, hundreds of secondary electrons are produced by the heavily ionizing fragments[5] and the efficiency can then reach 100%. The absence of parallax, which is due to the small thickness of the layers, the low sensitivity to γ-rays, and the high accuracy of the MWPC, makes this approach to slow neutron detection extremely attractive when compared to all other existing techniques.

Another possible application worth mentioning is connected with the detection of the electrons in electron microscopes. Several groups have considered using drift chambers or multiwire chambers for this purpose. A secondary-emission layer is attractive for two reasons: it is very thin and the accuracy does not depend on the angle; and it has to be in vacuum on the emission side, which makes it mechanically much more easy for electron microscopes since the impinging electrons have also to travel in vacuum.

We are thus faced with a task that is of considerable interest, and which will require much development if we are to exploit all the potential promises of these first results.

REFERENCES

1) M. Breidenbach, F. Sauli and R. Tirler, Nuclear Instrum. Methods 108, 23 (1973).

2) B. Sadoulet and B. Makowski, Space charge effects in multiwire proportional counters, CERN DPH II/PHYS 73-3 (1973).

3) A. Breskin, G. Charpak, F. Sauli, M. Atkinson and G. Schultz, Nuclear Instrum. Methods 124, 189 (1975).

4) See, for example, L.B. Loeb, Basic processes of gaseous electronics (University of California Press, Berkeley, 1961), p. 22 and p. 400.
Also, J.L. Pack and A.V. Phelps, Phys. Rev. 121, 798 (1961).

5) M.P. Lorikian, Nuclear Instrum. Methods 122, 377 (1974).

6) J.C. Faivre, H. Fanet, A. Garin, J.P. Robert, M. Rouger and J. Saudinos, IEEE Trans. Nuclear Sci. NS-24, 299 (1977).

7) J.C. Faivre, H. Fanet, A. Garin, J.P. Robert, M. Rouger and J. Saudinos, Compte-rendu d'activité, Note CEA-N-2026, p. 262 (1978).

8) J. Fischer and S. Shibata, Proc. Internat. Symp. on Nuclear Electronics, Versailles, 1968 (Documentation française, Paris, 1969), Vol. 3, p. 2-1.

9) J. Fischer and S. Shibata, Nuclear Instrum. Methods 101, 401 (1972).

10) V. Böhmer, Nuclear Instrum. Methods 107, 157 (1973).

11) G. Charpak, G. Petersen, A. Policarpo and F. Sauli, Nuclear Instrum. Methods 148, 471 (1978).

12) G. Charpak, G. Petersen, A. Policarpo and F. Sauli, IEEE Trans. Nuclear Sci. NS-25, 122 (1978).

13) J. Fischer, H. Okuno and A.H. Walenta, Spatial distribution of the avalanches in proportional counters, submitted to Nuclear Instrum. Methods (August 1977). Also BNL 23163.

14) T. Aoyama and T. Watanabe, Nuclear Instrum. Methods 150, 203 (1978).

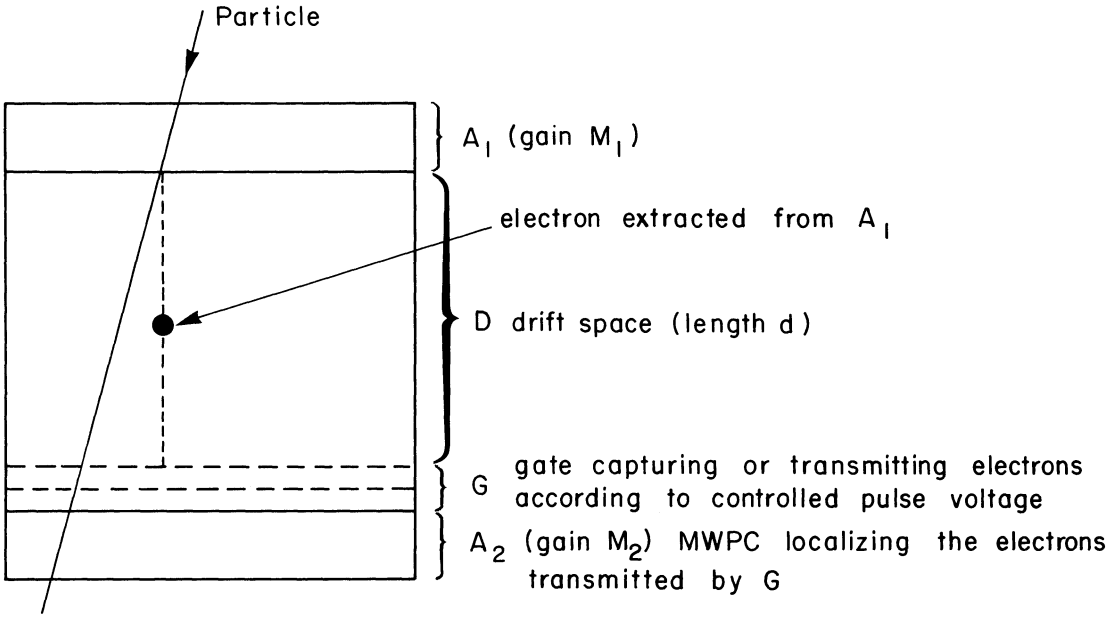

Fig. 1 Principle of gated multistep detector. The amplification M_2 of the MWPC A_2 is decreased by a factor M_1 with respect to normal gain $M = M_1 \cdot M_2$. The electrons liberated in the gap A_1 are preamplified by a factor M_1 and then transferred to A_2, after drifting in the space D for a time T_D, under the control of the gate G. The density per unit length of the electrons produced in A_1 is much higher than the density of ionization produced in the gas of D or A_2; conditions are set such that A_2 detects only the preamplified electron bunch. The electronic gate G opens only for preselected events; if their number is much smaller than the over-all particle flux, the space-charge reduction is roughly equal to M_1.

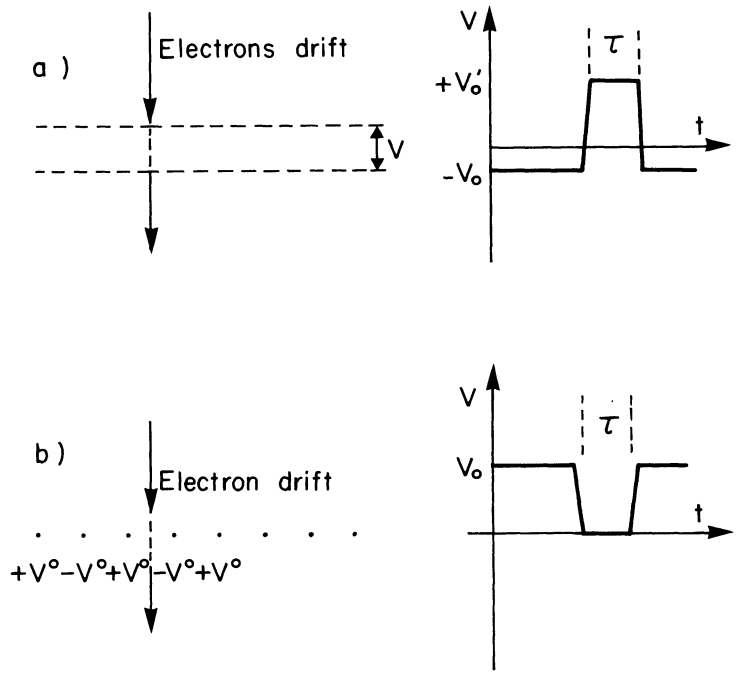

Fig. 2 Two possible solutions for the electric gating function G. In Fig. 2a two fine wire meshes are normally polarized, so as to stop all drifting electrons. Inversion of the applied potential for a time τ allows the electrons to cross the gap during the gating time. In Fig. 2b, instead, the gating function is obtained by a single grid of parallel wires at alternate potentials, transparency is restored by a voltage pulse that brings all wires to the same potential. Both methods have been tested in a prototype chamber with encouraging results.

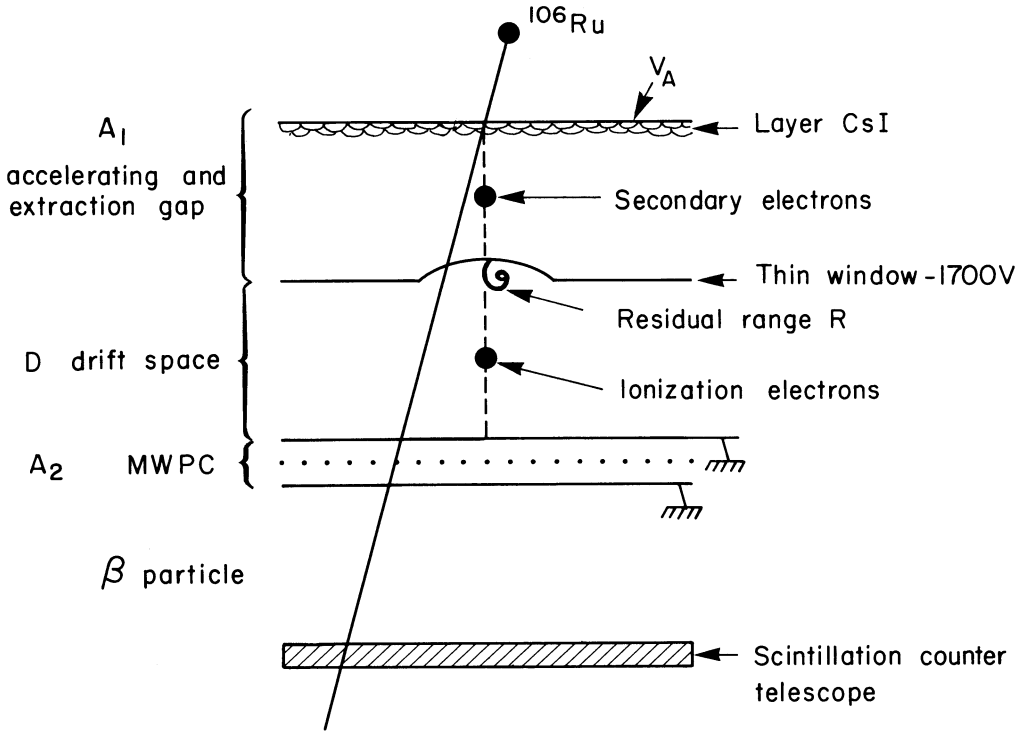

Fig. 3 Preamplification by secondary emission and acceleration of electrons. A secondary emission layer of CsI produces electrons in vacuum (10^{-3} Torr) when traversed by charged particles. A voltage up to 30 kV can be applied to the accelerating gap; the emitted electrons therefore receive enough energy to penetrate in the drift space, through a window of 2.5 μm aluminized mylar. The density of ionization of the electrons with the residual range R is much higher than the density along the primary trajectory. CsI layer of 150 μm, 1% density, on 40 μm of Al. Vacuum gap: 33 mm. Total drift length: 34 mm.

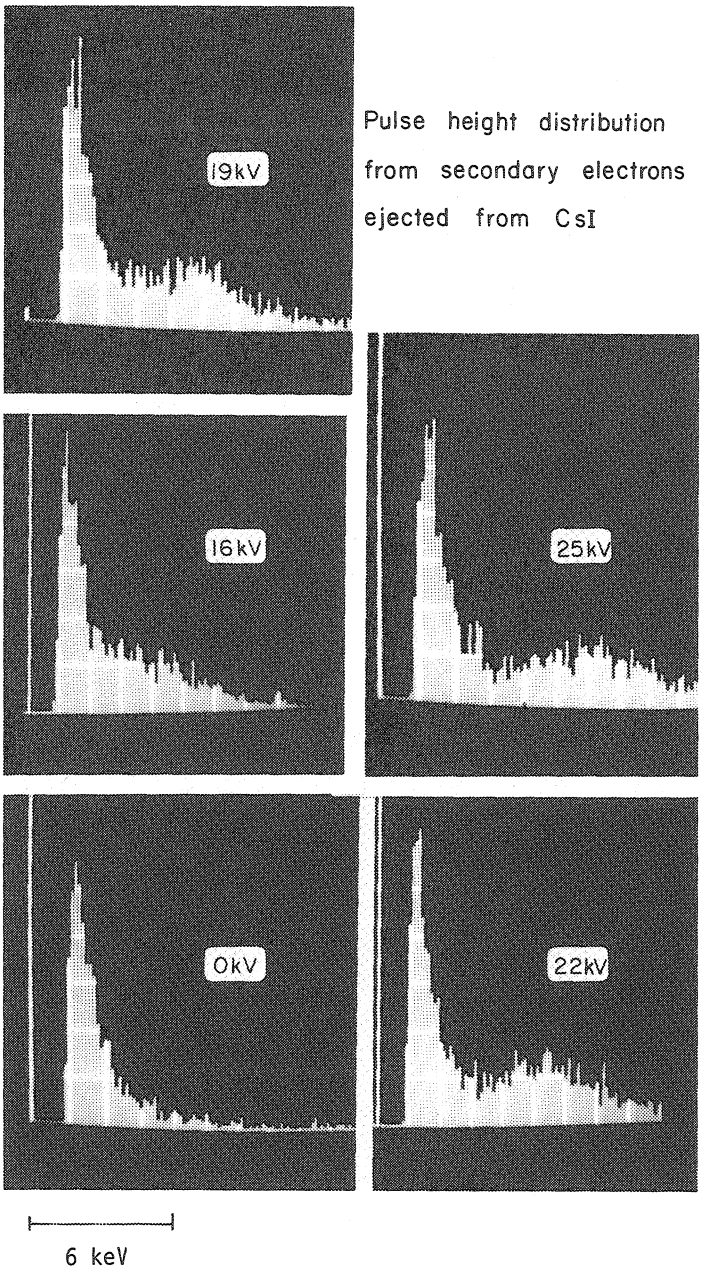

Pulse height distribution from secondary electrons ejected from CsI

Fig. 4 Pulse-height spectra of the delayed pulse observed in the chamber of Fig. 3, at variable accelerating potentials, and for secondary electrons ejected by β particles. The peak at 25 keV corresponds to an energy loss of 10 keV compatible with the residual energy of a single accelerated electron.

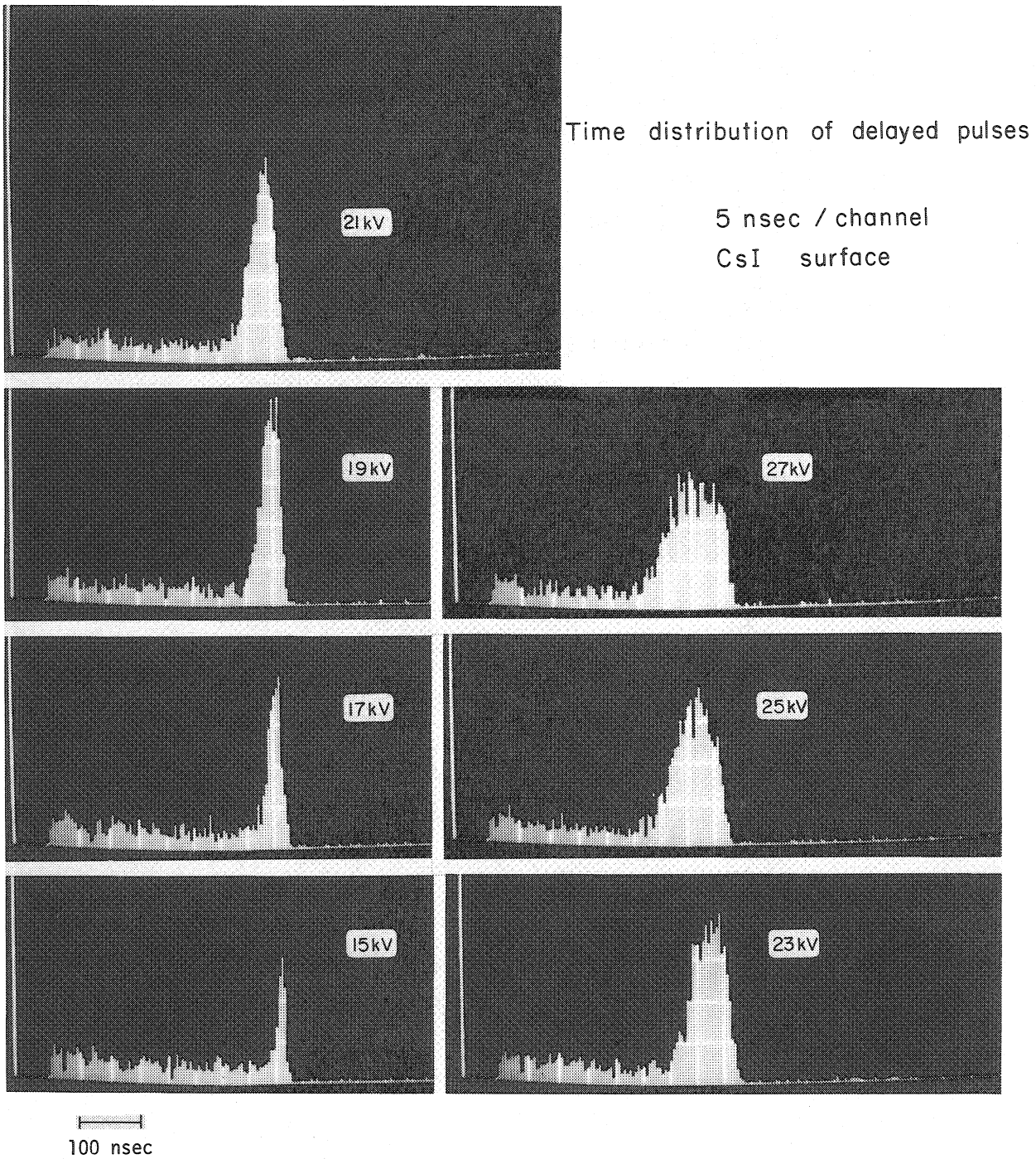

Fig. 5 Time delay of the secondary electrons measured in the chamber shown in Fig. 3. With the increase of the acceleration voltage V_A the secondary electrons penetrate more deeply into the drift space and are detected at shorter times. The horizontal scale corresponds to 5 nsec per division, with arbitrary origin; the background of events outside the peaks is generated by accidental triggers on the primary ionization electrons.

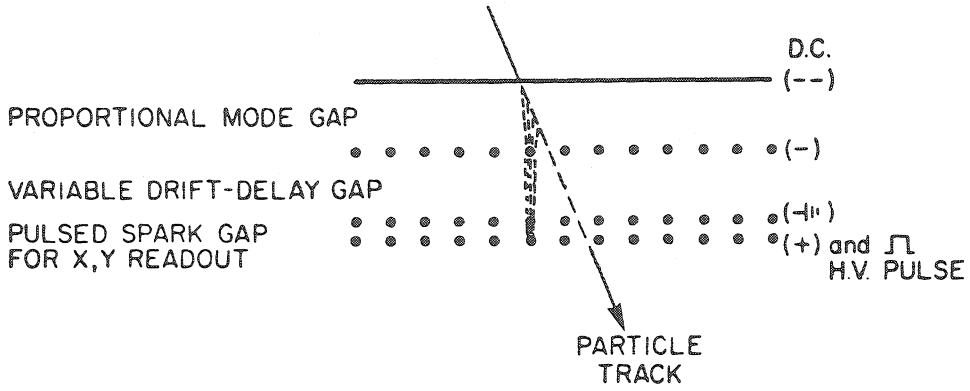

Fig. 6 The hybrid proportional and spark chamber. This figure, taken from Ref. 9, illustrates the supposed mechanism. Primary electrons give rise to an avalanche around the wires of the first plane; the electrons from the avalanche are transferred to the spark chamber via a drift space.

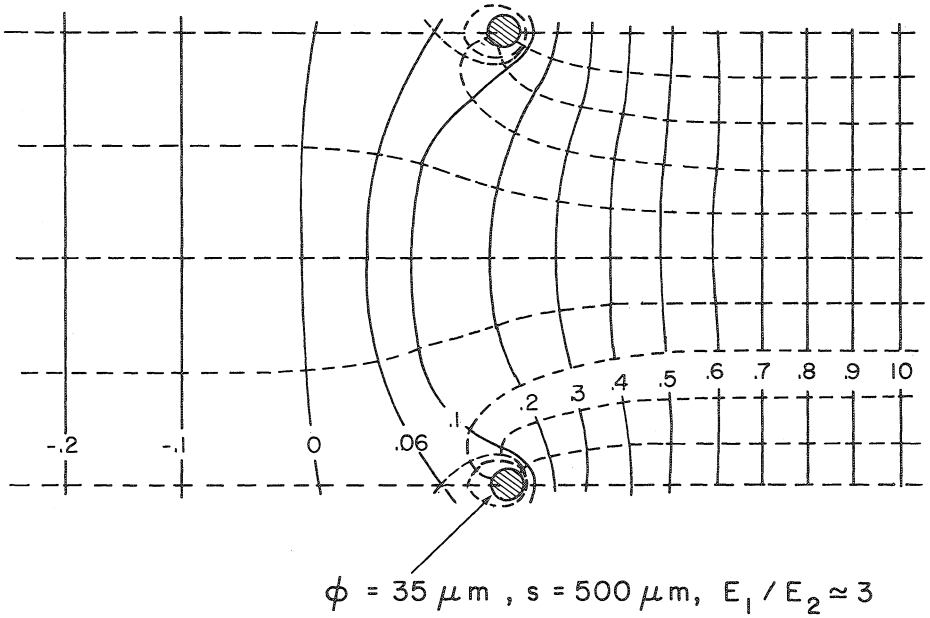

Fig. 7 Field lines and equipotentials around the preamplifying wires of a structure such as the one shown in Fig. 6. A set of parallel 35 μm diameter wires, 500 μm apart, separate a high-field region (E_1) from a transfer region (E_2). The ratio of fields in the two sections is a factor of three. As described in the text, the structure acts simply as a parallel-grid proportional counter with leaking-out field lines.

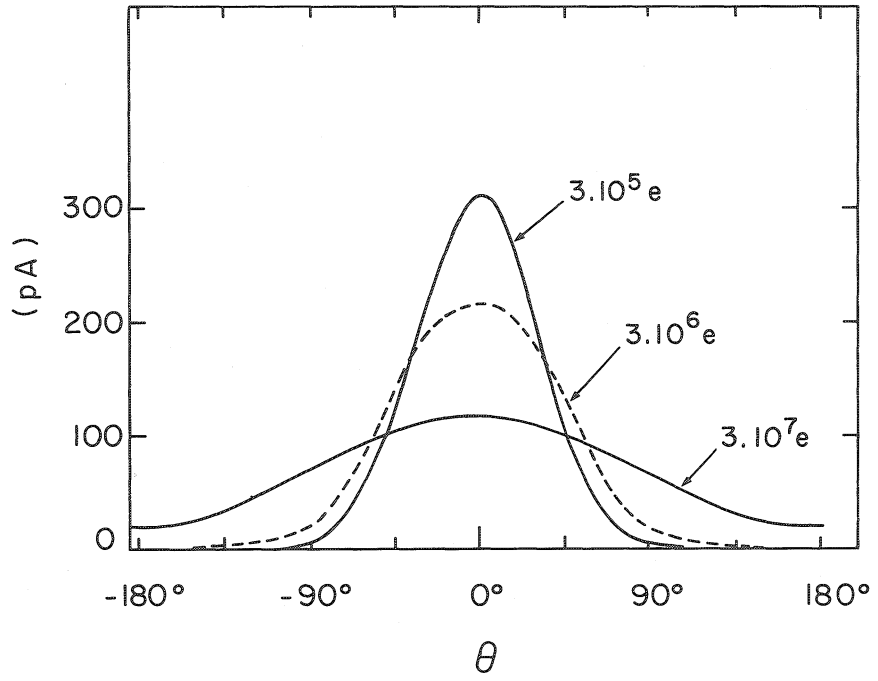

Fig. 8 Angular distribution of the ions around an anode wire. The angular distribution of the ion densities following an avalanche started by localized electrons in a cylindrical counter with wire thickness = 20 μm, cathode diameter = 1 cm, and gas filling: argon (94%), CO_2 (6%), bubbling through ethyl alcohol at 0°C. The curves represent the distribution for three values of the collected charge. Initial electron charge about 300 e.

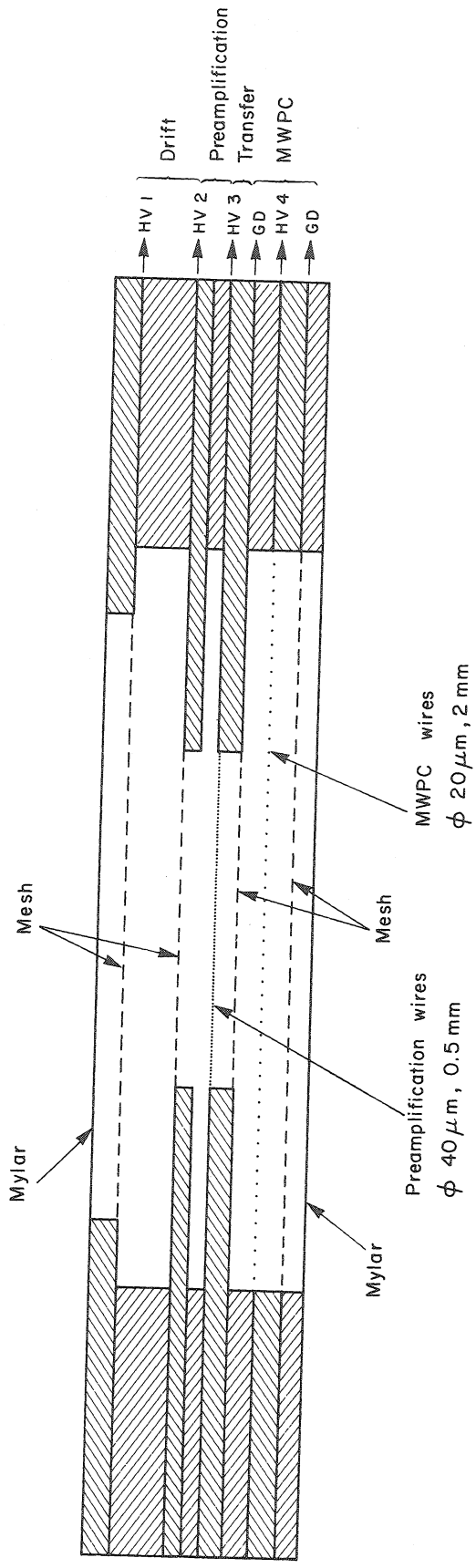

Fig. 9 Schematic cross-section of a test multi-step proportional chamber, using the hybrid chamber concept to implement the preamplification function. Electrons are multiplied in the preamplification gap, and some of them are transferred to the MWPC. The addition of a drift space in front of the preamplification gap greatly improves the chamber energy resolution for neutral radiation, although it appears that it is not essential for the efficient detection of fast charged particles.

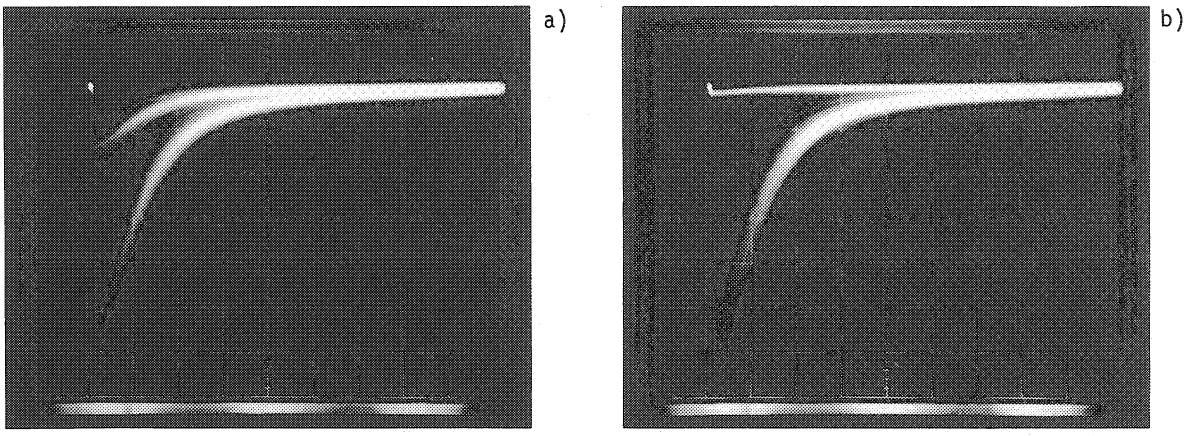

Fig. 10 Separation of direct and preamplified pulses induced by 5.9 keV X-rays, detected directly in the MWPC and after preamplification by a factor close to 25. Vertical scale: 20 mV/div. (a) and 200 mV/div. (b); horizontal scale 1 μsec/div. A charge amplifier with a sensitivity of 250 mV/pC and a 2 μsec time constant has been connected to the chamber.

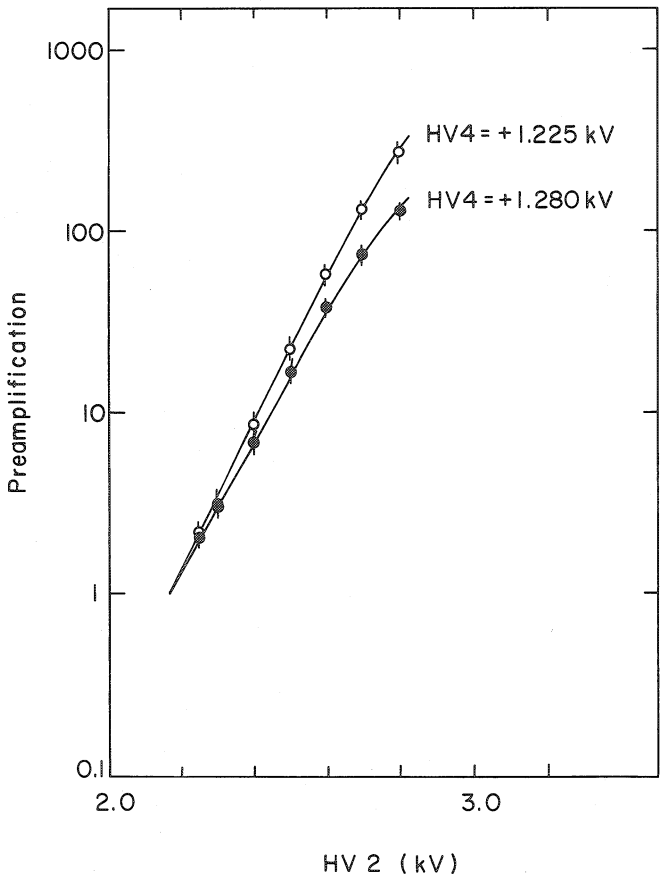

Fig. 11 Measured preamplification factor for ^{55}Fe X-rays as a function of the preamplification grid voltage for two values of the MWPC potential. The error bars around the measured points represent the FWHM of the pulse-height distribution of the detected 5.9 keV line. The chamber shown in Fig. 9 was operated in a gas mixture obtained by bubbling pure argon through ethyl alcohol at 0°C.

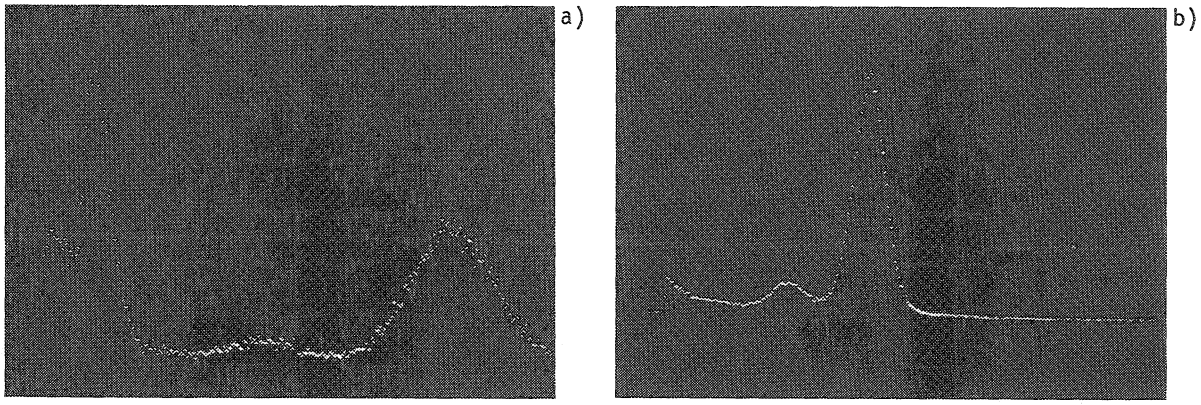

Fig. 12 Pulse-height spectra from ^{55}Fe X-rays, measured just above threshold for preamplification (a), and after preamplification by a factor of about 40 (b). The horizontal scale is arbitrary and is different in the two pictures.

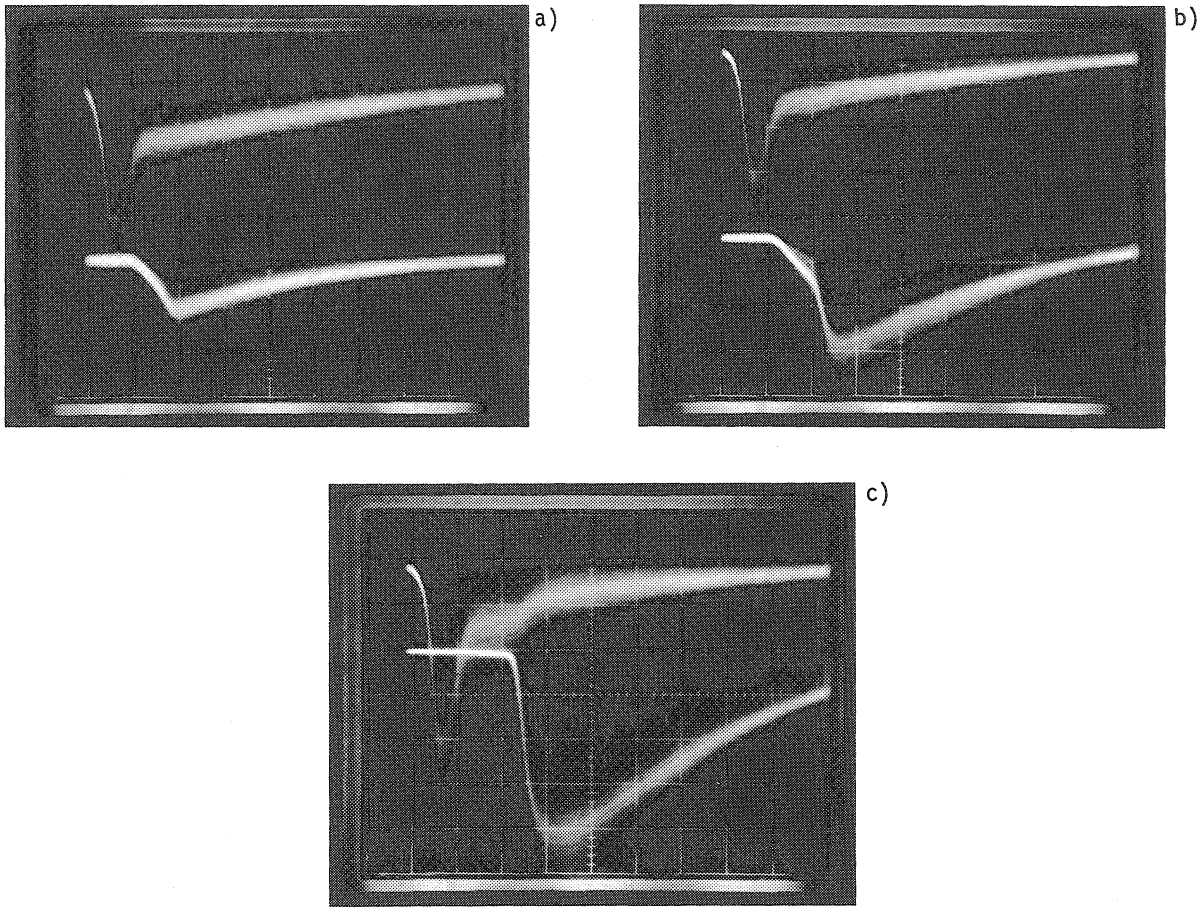

Fig. 13 At high preamplification factors (about 100) a signal can be detected directly on the preamplification grid, as shown in the upper traces in all pictures. The lower traces show the charge detected in coincidence on the MWPC operated in a pure collection mode (a), at the beginning of proportional multiplication (b), and in full operation (c). The vertical sensitivities are 4 mV/div. in all pictures, except for the lower trace in (c) where it has been decreased to 100 mV/div.; the horizontal scale is 200 nsec/div. The charge amplifier described in the text has been used to obtain the pictures.

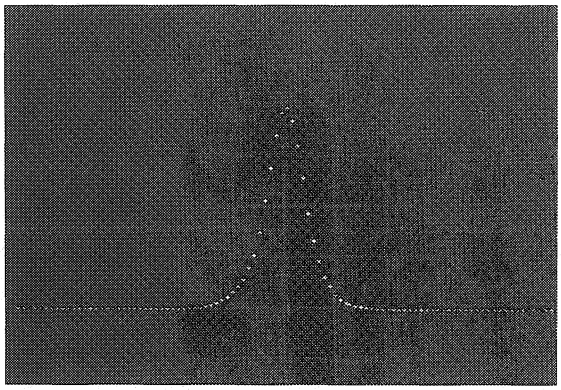

Fig. 14 Time jitter measured at fixed discrimination threshold (∿ 0.1 pC on the chamber) between the fast preamplified pulse (upper trace in Figs. 13) and the delayed pulse detected in the proportional chamber, for ^{55}Fe X-rays. The horizontal scale is 10 nsec/div.

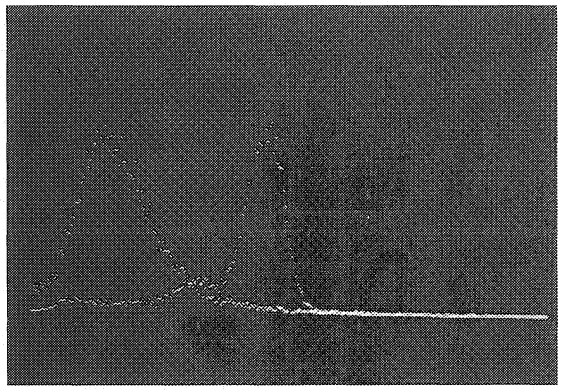

Fig. 15 Comparison of pulse-height spectra on the preamplified charge at a preamplification factor of about 100, for ^{55}Fe X-rays and minimum ionizing electrons.

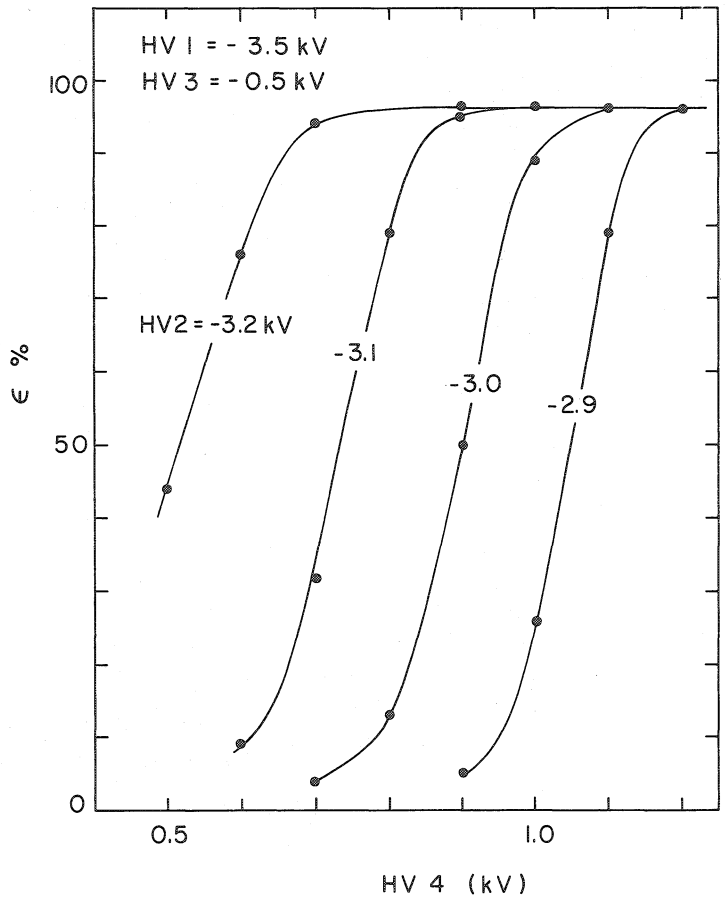

Fig. 16 Detection efficiency for fast electrons, at a fixed discrimination threshold on the proportional chamber (∿ 0.1 pC at the wires), as a function of anodic potential, and for several values of the preamplification grid voltage. When using a radioactive β emitter for this kind of measurement, it is usually impossible to reach 100% efficiency.

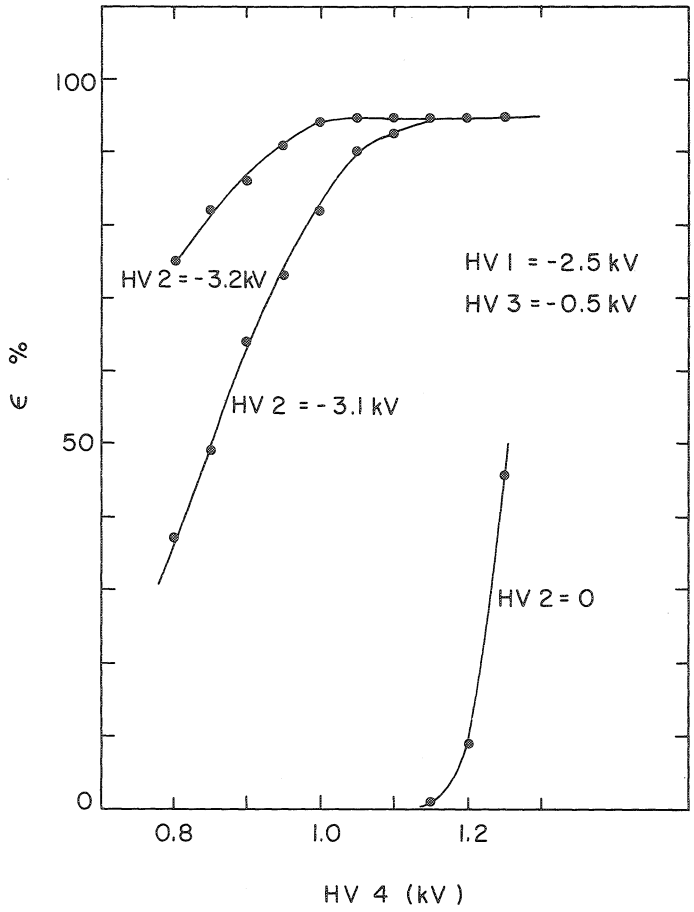

Fig. 17 Efficiency for the detection of fast electrons, in the conditions of Fig. 16 except for an inversion of electric field in the upper drift region (see Fig. 9). It appears that for charged particles full efficiency can be obtained on the preamplified tracks even without the addition of the first drift section. The efficiency of detection of the direct (non-preamplified) section of the track is also shown (curve $HV_2 = 0$).

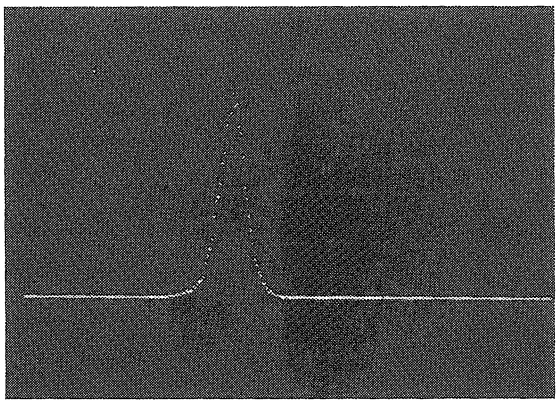

Fig. 18 Time resolution for charged-particle detection. Time jitter distribution between detection of ^{106}Ru β-particles by a scintillation telescope and by the MWPC after preamplification. Mixture of argon-CO_2 (97%, 3%) bubbling through alcohol at 0°C. FWHM = 20 nsec. Horizontal scale 50 nsec/div.